Thermal weakening localizes intraplate deformation along the southern Australian continental margin

Simon P. Holford[1], Richard R. Hillis[1], Martin Hand[1] & Mike Sandiford[2]

[1]*Centre for Tectonics, Resources and Exploration (TRaX), University of Adelaide, SA 5005, Australia (simon.holford@adelaide.edu.au)*

[2]*School of Earth Sciences, University of Melbourne, VIC 3010, Australia*

ABSTRACT

The southern Australian continental margin has been undergoing mild active deformation over the past ~10 Myr, manifested today by unusually high levels of seismicity for a relatively stable intraplate region. However, this deformation is markedly partitioned, with zones of abundant neotectonic structures, enhanced relief and high seismicity such as the Flinders Ranges and Southeastern Highlands separated by areas of little neotectonic activity, subdued topography and low levels of seismicity such as the Murray and Eucla basins. We have made a new compilation of heat flow data for the southern margin comprising 192 measurements. This new database shows that variations in heat flow correlate well with the distribution of neotectonic structures and historical record of seismicity, with regions of active deformation corresponding to elevated heat flows of up to ~90 mWm^{-2}. We propose that the southern Australian margin provides the best evidence to-date that active intraplate deformation may be localized by the thermal properties of the crust and upper mantle.

KEYWORDS

Intraplate deformation, heat flow, neotectonics, seismicity, reactivation, Australia.

INTRODUCTION

Plate tectonic theory readily accounts for deformation of plate boundaries but does not satisfactorily explain deformation and seismicity of plate interiors. Various studies have identified the thermal state of the crust and mantle as the dominant control on intraplate lithospheric strength (Kusznir and Park, 1982; Sonder and England, 1986), but there are few examples where localized thermal weakening of the lithosphere is demonstrably responsible for localizing intraplate deformation. Liu and Zoback (1997) proposed that thermal weakening could explain the anomalously elevated seismicity of the intraplate New Madrid Seismic Zone (NMSZ), Missouri, which witnessed three M>7 earthquakes in 1811-1812, on the basis of elevated heat flow within the NMSZ (~60 mW m^{-2}) compared to background levels in the central-eastern United States (~45 mW m^{-2}). Using 1D numerical models of lithospheric strength, Liu and Zoback (1997) showed that the heat flow observed in the NMSZ is sufficient to weaken the underlying lower crust and upper mantle and focus intraplate stresses in the upper crust, thereby localizing seismicity and deformation. Subsequent investigations of the NMSZ have revealed a much smaller heat flow anomaly (~3 mW m^{-2}), implying that the lithospheric strength of the NMSZ is essentially the same as that of surrounding regions (McKenna et al., 2007). NMSZ seismicity has most recently been attributed to migrating seismicity across zones of similarly reduced strength e.g. failed rifts (McKenna et al., 2007), but the question of the extent to which intraplate deformation and reactivation may be localized by the thermal architecture of the lithosphere remains open.

Whereas clear relationships between thermal weakening of the lithosphere and localized intraplate deformation have been difficult to establish, the geological record contains numerous examples of structural reactivation during episodes of intraplate orogeny and basin inversion (e.g. Holdsworth et al., 1997), leading to the viewpoint that pre-existing zones of mechanical weakness (e.g. faults, shear zones, failed rifts and compositional boundaries) exert the first-order control on the localization of intraplate deformation (Sykes, 1978). However, relatively little attention has been paid to instances where regions containing structures favorably orientated for reactivation exhibit no record of neotectonic activity or historical seismicity.

Here we examine the controls on localized intraplate deformation along the southern Australian continental margin, which shows strong spatial partitioning of neotectonic and seismic activity. Through comparison with a new compilation of 192 surface heat flow measurements (Fig. 1), we show that strong correlations exist between regions of neotectonic faulting, enhanced seismicity and elevated heat flow at length-scales of 100-1000 km. We believe that while mechanical weakness may control the deformation within a region, thermal weakening of the lithosphere is the primary control on which regions are prone to deformation.

ACTIVE TECTONICS OF THE SOUTHERN AUSTRALIAN MARGIN

Australia is amongst the most active 'stable continental regions' with a seismic moment release rate of order 10^{-17}-10^{-16} s^{-1} (Célérier et al., 2005), several times higher than comparable intraplate regions (e.g. Europe, Africa; Sandiford and Egholm, 2008). Much of the seismicity occurs along the southern Australian continental margin, which formed following Cretaceous-Paleogene breakup with Antarctica and has markedly heterogeneous basement geology characterized by numerous Archaean-Paleozoic terranes (Teasdale et al., 2003). Present-day seismicity is partitioned into several distinct seismic zones, separated by regions with considerably fewer earthquakes (Leonard, 2008). Most contemporary seismic activity in south-central Australia occurs in the Flinders seismic zone (FSZ) (Fig. 1) which corresponds with the topographically elevated Flinders and Mt Lofty Ranges, and the eastern Eyre Peninsula, where earthquakes as large as M_S ~6 have been recorded (Célérier et al., 2005) (Fig. 2). There is also a ~SW-NE trending region of elevated seismicity termed the southeast seismic zone (SESZ) that extends from the Otway Basin and largely overlaps with the elevated topography of the Southeastern Highlands. Tasmania is also associated with high seismicity. Between the FSZ and the SESZ is an area of markedly reduced earthquake activity corresponding to the Murray Basin. To the west of the FSZ, the number of recorded earthquakes dramatically reduces in the Eucla and Bight Basins, before increasing in the Yilgarn Craton west of ~128°E.

The distribution of seismicity shows remarkable correspondence with the neotectonic record of the southern Australian margin (Fig. 1). The Flinders and Mt Lofty Ranges have been undergoing uplift due to ~E-W shortening over the past 10 Myr (Célérier et al., 2005), and palaeoseismic studies of Quaternary faults that bound the ranges have estimated slip rates of 20-100 m Myr^{-1} and maximum magnitude earthquake events of M_W ~7.3 (Quigley et al., 2006). In SE Australia, Miocene and older sediments have been deformed by folding and reverse faulting induced by approximately NW-SE crustal shortening from the late Miocene onwards (Sandiford, 2003). This deformation is partly responsible for the Otway and Strzelecki Ranges and the Simpson and Fergusons Hill anticlines (Sandiford, 2003). STRM images of the Southeastern Highlands reveal numerous NNE and ENE-trending faults, along which reverse movements of up to several hundred metres have contributed to Pliocene-onwards uplift (Holdgate et al., 2008).

In contrast, there are relatively few compressional structures in the topographically-subdued and seismically-quiet Murray Basin (Sandiford, 2003). Identifiable structures include the

Cadell Fault, displacement along which diverted the Murray River ~50 Ka, but the density of active faulting is considerably lower than in the adjoining, topographically elevated regions (Sandiford, 2003). Likewise, there are significantly fewer compressional structures identified in the onshore Eucla and offshore Bight basins where seismicity levels are amongst the lowest of any part of the continent (Hillis et al., 2008). The Eucla Basin contains the vast Nullabor Plain, a marine limestone terrace >1000 km long that was exposed ~15 Myr ago by long-wavelength uplift of the southern Australian margin (Sandiford, 2007). STRM images across the Nullabor Plain reveal a number of linear north-south trending faults, but maximum displacements on these structures are generally ~10 m, considerably lower than inferred for faults bounding the Flinders and Mt Lofty Ranges (Hillis et al., 2008).

The orientations of neotectonic structures along the southern margin are generally consistent with an E-W to SE-NW orientated S_{Hmax} controlled by plate boundary forces (Hillis et al., 2008). Basement structure maps of the southern margin (e.g. Teasdale et al., 2003) reveal highly anisotropic basement dissected by faults and shear zones, and show numerous NE-SW and N-S trending structures in the Murray, Bight and Eucla basins that should be suitably oriented for failure in the *in situ* stress field. The absence of neotectonic structures and low levels of seismicity in these regions imply an additional, regional control on localization of deformation. Dyksterhuis and Muller (2008) proposed that rheological contrasts between geological provinces and evolving plate boundary forces could explain strain localization, whilst Célérier et al. (2005) noted a correlation between the spatial extents of the FSZ and the South Australian Heat Flow Anomaly (SAHFA), a zone of elevated heat surface flow (average 92 ± 10 mW m^{-2}) (Neumann et al., 2000), and thus attributed active intraplate deformation to thermal weakening.

COMPARING PRESENT-DAY HEAT FLOW AND DISTRIBUTION OF INTRAPLATE DEFORMATION

We have compiled a new map of the surface heat flow (Q (mW m^{-2})) of the southern Australian margin, based on 192 measurements comprising published data (e.g. Cull, 1982; Goutorbe et al., 2008; Fig. 1) and recently reported estimates from geothermal exploration (Table DR1). Data density is greatest in regions of active petroleum/mineral/geothermal exploration (e.g. Flinders Ranges and Otway Basin). Measurements are sparser in the Eucla and Bight basins, but the quality of these estimates is generally good (Cull, 1982). Small-scale heat flow anomalies can result from groundwater flow (McKenna et al., 2007), and this is thought to contribute to elevated geothermal gradients observed in parts of central Australia, but the majority of measurements from the southern margin are thought to reflect crustal properties (Neumann et al., 2000).

Our map provides better definition of individual heat flow provinces than previous Australian heat flow maps (e.g. Cull, 1982; Fig. 2). Heat flow increases from west to east along the margin, from values of ~35-40 mW m^{-2} at longitudes <125°E to mostly >80 mW m^{-2} between 135 and 150°E, but some notable short-wavelength variations are superimposed on this regional pattern. Heat flow locally exceeds >100 mW m^{-2} in the Flinders Ranges, Tasmania and western parts of the southeastern Highlands. There are noticeable reductions in heat flow within the Murray and Bight/Eucla basins, with reported values 30-50 mW m^{-2} lower than adjacent regions.

The spatial variation of heat flow and distribution of neotectonic structures and historical seismicity show a remarkable degree of correspondence (Figs. 1, 2). Regions of high heat flow such as the Flinders Ranges, Southeastern Highlands and Tasmania are characterized by relatively high seismicity, whilst the Murray and Bight/Eucla basins experience few earthquakes. STRM 3 arcsecond images of the Eyre Peninsula-Flinders/Mt Lofty Ranges illustrate these associations well (Fig. 3). The Flinders and Mt Lofty Ranges, Yorke Peninsula and eastern Eyre Peninsula (heat flow >80 mW m^{-2}) are flanked by numerous faults that displace Pliocene-Quaternary rocks (e.g. Quigley et al., 2006) and have witnessed frequent *M*>5 earthquakes. In the western and northern Eyre Peninsula (heat flow <60 mW m^{-2}) there is little recorded seismicity and few neotectonic features have been recognized, despite this region containing numerous NE-SW basement structures favorably oriented for reactivation under the prevailing NW-SE to W-E S_{Hmax}.

To evaluate the relationship between surface heat flow and ongoing deformation, we compared average heat flow with the amount of seismic energy released by earthquake activity for eighteen 3° x 3° cells along the margin. We utilized a comprehensive catalogue of Australian earthquakes between 1900 and 2007 (Leonard, 2008). After screening to remove aftershocks and duplicates (Appendix DR1), we estimated the amount of seismic energy released in each 3° x 3°cell using an empirical relationship that relates seismic energy to earthquake magnitude:

$$\log E_S = 1.5M_S + 4.8$$

where E_S is the radiated seismic energy (Joules) and M_S is the measured surface wave magnitude (Scholz, 2002).

Figure 4 compares total seismic energy (TJ) with average heat flow (calculated using the smoothed grid presented in Fig. 2) for the eighteen 3° x 3° cells. There is a clear positive correlation between heat flow and seismic energy. The six cells that exhibit the greatest seismic energy release (>50 TJ) are in the FSZ and SESZ. In cells that cover the quiescent

Bight and Eucla basins, Q is ~48-55 mW m^{-2} and E_S is ~1-4 TJ. There are two major exceptions to the positive correlation between Q and E_S. Cells in the western part of the margin, exhibit unusually high levels of seismic activity at heat flow values of ~35-42 mW m^{-2}. In cell 10 covering the Murray Basin region, Q is ~73 mW m^{-2} but E_S is only ~1 TJ (the high value of Q for this cell is probably due to the 3° x 3° cell 'capturing' some of the elevated heat flow in the FSZ and SESZ). Excluding the Murray Basin and western cells where seismicity is anomalously low and high respectively, compared to the overall regional pattern, there is a correlation coefficient of 0.64 between Q and E_S. This is a surprisingly good result considering the ~100 year record of historical seismicity is several orders of magnitude shorter than recurrence intervals calculated for large (e.g. M>6) earthquakes in this region (Quigley et al., 2006), along with the many other geologic factors that may influence seismicity.

DISCUSSION

Our observations imply that at length-scales of 100-1000 km along the southern Australia margin, thermal weakening of the lithosphere controls the location of active intraplate deformation. High heat flows in the Flinders Ranges are due to the unusual abundance of heat producing elements (HPEs) in Palaeoproterozic-Meosoproterozoic basement, witnessed by heat production rates >10 μW m^{-3}(Neumann et al., 2000). The ~30 mW m^{-2} difference in heat flow between the Flinders Ranges and surrounding regions (e.g. Murray Basin, Eyre Peninsula) implies that Moho temperatures could be ~90-120°C hotter beneath the former (depending on the length-scale of the thermal anomaly), sufficiently high to reduce bulk lithosphere strength by a factor of 2-5 and focus deformation (Célérier et al. 2005). Shear wavespeeds at 100 km depth beneath the Bight/Eucla and Murray basins are ~5% faster than beneath the Flinders/Mt Lofty Ranges and Southeastern Highlands (Fishwick et al., 2008), which implies that the lithosphere at 100 km beneath the deforming regions may be >100°C hotter (Goes et al., 2000). Sandiford and Egholm (2008) show that Moho temperature variations as small as 10-30°C may explain the elevated levels of seismicity observed along southwestern parts of margin, due to steady-state heat flow across the oceanic-continental lithospheric step. The observation that the seismicity of the Southeastern Highlands broadly parallels the architecture of the continental margin and crosscuts underlying structural trends (Teasdale et al., 2003) suggests that lateral heat flow may also play a role in localizing that deformation.

We do not wish to imply that thermal weakening can fully explain localization of the intraplate seismicity and neotectonic deformation along the southern Australian margin. As in many intraplate settings factors such as pre-existing structural weaknesses and zones of overpressured crust probably play an important role in the distribution of deformation (Holdsworth et al., 1997). However, we believe that the potential for localization of deformation by the thermal architecture of the crust and lithosphere is often overlooked, especially at the terrane scale, because reactivation of pre-existing zones of structural weakness is usually invoked. There is growing support for the thermal properties of the crust exerting a first-order control on focussing intraplate deformation from studies around the world. Stephenson et al. (2009) have shown that intraplate deformation in cold lithosphere (~45 mW m^{-2}) in southeastern Ukraine preferentially occurs in the >20 km thick Dniepr-Donets Basin as a consequence of thermal refraction stemming from bulk thermal conductivity in the sedimentary basin that is lower than adjacent crystalline basement. Similarly, in Central Australia Hand and Sandiford (1999) postulated that spatial and temporal variation in thermal weakening of the lithosphere due to shifting subsidence patterns exerted a modulating effect on the pattern of basement fault reactivation during intraplate orogeny.

CONCLUSION

The distribution of neotectonic structures and present-day seismicity along the southern Australian margin shows a strong correspondence with the pattern of surface heat flow, implying that thermal weakening has localized intraplate deformation. We propose that in this, and potentially other intraplate settings, the thermal properties of the crust and upper mantle exert a regional-scale (100-1000 km) modulating control on which parts of the lithosphere undergo failure and which parts experience relatively less deformation.

Acknowledgments

We thank Mark Leonard for providing access to Geoscience Australia’s earthquake database. This work was supported by ARC Discovery Projects DP0879612 and DP055613 and forms TRaX Record #XX.

References

Célérier, J., Sandiford, M., Hansen, D.L., and Quigley, M., 2005, Modes of active intraplate deformation, Flinders Ranges, Australia: Tectonics, v. 24, TC6006, doi:10.1029/2004TC001679.

Cull, J.P., 1982, An appraisal of Australian heat-flow data: BMR Journal of Australian Geology and Geophysics, v. 7, p. 11-21.

Dyksterhuis, S., and Müller, R.D., 2008, Cause and evolution of intraplate orogeny in Australia: Geology, v. 36, p. 495-498, doi:10.1130/G24536A.1.

Fishwick, S., Heintz, M., Kennett, B.L.N., Reading, A.M., and Yoshizawa, K., 2008, Steps in lithospheric thickness within eastern Australia, evidence from surface wave tomography: Tectonics, v. 27, TC4009, doi:10.1029/2007TC002116.

Goes, S., Cammarano, F., and Hansen, U., 2000, Shallow mantle temperatures under Europe from P and S wave tomography: Journal of Geophysical Research, v. 105B, p. 11,153-11,169.

Goutorbe, B., Lucazeau, F., and Bonneville, A., 2008, Surface heat flow and the mantle contribution on the margins of Australia: Geochemistry, Geophysics, Geosystems, v. 9., Q05011, doi:10.1029/2007GC001924.

Hand, M., and Sandiford, M., 1999, Intraplate deformation in central Australia, the link between subsidence and fault reactivation: Tectonophysics, v. 305, p. 121-140.

Hillis. R.R., Sandiford, M., Reynolds, S.D., and Quigley, M.C., 2008, Present-day stress, seismicity and Neogene-to-Recent tectonics of Australia's 'passive' margins: intraplate deformation controlled by plate boundary forces, *in* Johnson, H., et al., eds., The nature and origin of compression in passive margins: Geological Society of London Special Publication 306, p. 71-90, doi:10.1144/SP306.3.

Holdgate, G.R., Wallace, M.W., Gallagher, S.J., Wagstaff, B.E., and Moore, D., 2008, No mountains to snow on: major post-Eocene uplift of the East Victoria highlands; evidence from Cenozoic deposits: Australian Journal of Earth Sciences, v. 55, p. 211-234, doi:10.1080/08120090701689373.

Holdsworth, R.E., Butler, C.A., and Roberts, A.M., 1997, The recognition of reactivation during continental deformation: Geological Society [London] Journal, v. 154, p. 73-78.

Kusznir, N.J., and Park, R.G., 1982, Intraplate lithosphere strength and heat flow: Nature, v. 299, p. 54-542.

Leonard, M., 2008, One hundred years of earthquake recording in Australia: Bulletin of the Seismological Society of Australia, v. 98, p. 1458-1470, doi:10.1785/0120050193.

Liu, L., and Zoback, M.D., 1997, Lithospheric strength and intraplate seismicity in the New Madrid seismic zone: Tectonics, v. 16, p. 585-595.

McKenna, J., Stein, S., and Stein, C.A., 2007, Is the New Madrid seismic zone hotter and weaker than its surroundings?, *in* Stein, S., and Mazzotti, S., ed., Continental Intraplate Earthquakes: Science, Hazard, and Policy Issues: Geological Society of America Special Paper 425, p. 167–175, doi:10.1130/2007.2425(12).

Neumann, N., Sandiford, M., and Foden, J., 2000, Regional geochemistry and continental heat flow: implications for the origin of the South Australian heat flow anomaly: Earth and Planetary Science Letters, v. 183, p. 107-120.

Quigley, M.C., Cupper, M.L., and Sandiford, M., 2006, Quaternary faults of south-central Australia: palaeoseismicity, slip rates and origin: Australian Journal of Earth Sciences, v. 53, p. 285-301, doi:10.1080/08120090500499271.

Sandiford, M.., 2003, Neotectonics of southeastern Australia: Linking the Quaternary faulting record with seismicity and in situ stress, *in* Hillis, R.R., and Muller, R.D., eds., Evolution and dynamics of the Australian plate: Geological Society of Australia Special Publication 22 and Geological Society of America Special Paper 372, p. 107-120.

Sandiford, M., 2007, The tilting continent: A new constraint on the dynamic topographic field from Australia: Earth and Planetary Science Letters, v. 261, p. 152-163, doi:10.1016/j.epsl.2007.06.023.

Sandiford, M., and Egholm, D.L., 2008, Enhanced intraplate seismicity across continental margins: some causes and consequences: Tectonophysics, v. 457, p. 197-208, doi:10.1016/j.tecto.2008.06.004.

Sonder, L., and England, P., 1986, Vertical averages of rheology of the continental lithosphere; relation to thin sheet parameters: Earth and Planetary Science Letters, v. 77, p. 81-90.

Stephenson, R., Egholm, D.L., Nielsen, S.B., and Stovba, S.M., 2009, Role of thermal refraction in localizing intraplate deformation in southeastern Ukraine: Nature Geoscience, v. 2., p. 290-293, doi:10.1038/NGEO479.

Scholz, C.H., 2002, The Mechanics of Earthquakes and Faulting: Cambridge University Press, Cambridge.

Sykes, L.R., 1978, Intraplate seismicity, reactivation of pre-existing zones of weakness, alkaline magmatism and other tectonism post-dating continental fragmentation: Reviews of Geophysics, v. 16, p. 621-688.

Teasdale, J.P., Pryer, L.L., Stuart-Smith, P.G., Romine, K.K., Etheridge, M.A., Loutit, T.S., and Kyan, D.M., 2003, Structural framework and basin evolution of Australia's southern margin: APPEA Journal, v. 43, p. 13-37.

FIGURE LEGENDS

Figure 1. Heat flow and neotectonics of the southern Australian margin. Note localization of neotectonic fault scarps (red) in regions such as the Flinders/ Mt Lofty Ranges and Southeastern Highlands, and relatively few structures in the Murray and Eucla basins. Neotectonic features after Hillis et al. (2008), Holdgate et al. (2008). Distribution of Flinders and Southeast seismic zones after Leonard (2008). Full details of references used to compile heat flow database provided in Table DR1. EP, Eyre Peninsula; FR, Flinders Ranges; MLR, Mt Lofty Ranges; OB, Otway Basin; YP, Yorke Peninsula.

Figure 2. Contoured (kriged) heat flow map with superimposed seismicity, demonstrating strong qualitative correlation between regions of high levels of heat flow and elevated seismicity, particularly along the southeastern margin. Map shows the eighteen 3° x 3° cells used in the quantitative comparison of heat flow and seismicity.

Figure 3. A. STRM 3 arcsecond image of area encompassing the southwestern Flinders and Mt Lofty Ranges and Eyre Peninsula, with superimposed heat flow, seismicity, regional S_{Hmax} orientations (Hillis et al., 2008)) and neotectonic fault scarps identified through interpretation of STRM data. Note density of faults (black) along the western Mt Lofty and Flinders Ranges, Yorke Peninsula and eastern Eyre Peninsula. There is a clear decrease in neotectonic structures and seismicity as heat flow decreases towards the central and western Eyre Peninsula. Gray features are faults identified from 1:250,000 geological maps that are favorably oriented for reactivation under present-day stress conditions but have no distinct topographic expression and thus inferred to be inactive. B. Uninterpreted STRM image of Mt Lofty Ranges east and north of Adelaide, South Australia, illustrating high quality of data used to identify neotectonic faults. C. Interpreted image highlighting neotectonic faults that bound Mt Lofty Ranges and Yorke Peninsula and displace Eocene-Holocene sediments of the Gulf St Vincent basin.

Figure 4. Comparison of average heat flow (mWm^{-2}) and seismic energy release (TJ) for the eighteen 3° x 3° cells. Average heat flow calculated by averaging values from the kriged grid at 30’ intervals. Seismic energy calculated from earthquakes in each cell that meet catalogue completeness levels (Appendix DR1).

Holford et al Figure 1

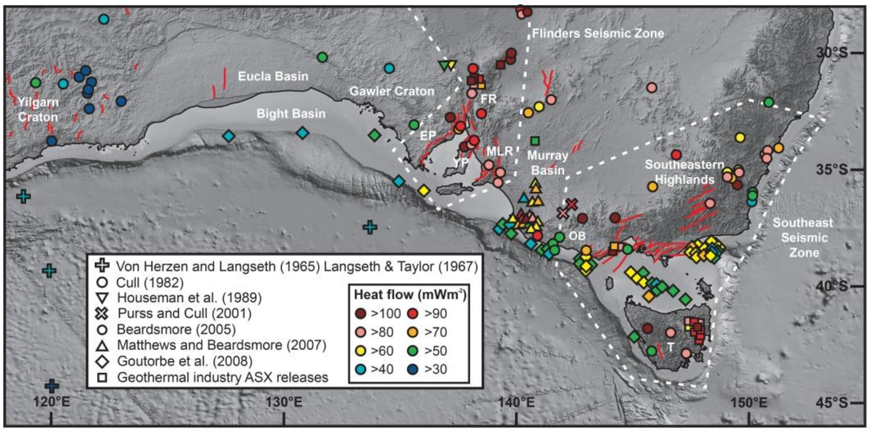

Holford et al Figure 2

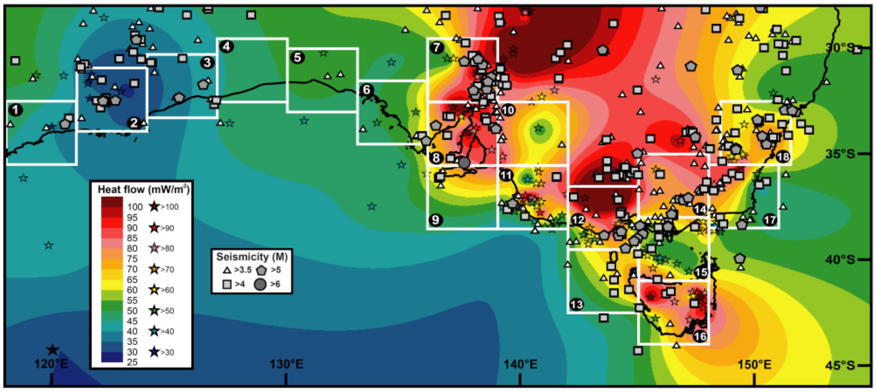

Holford et al Figure 3

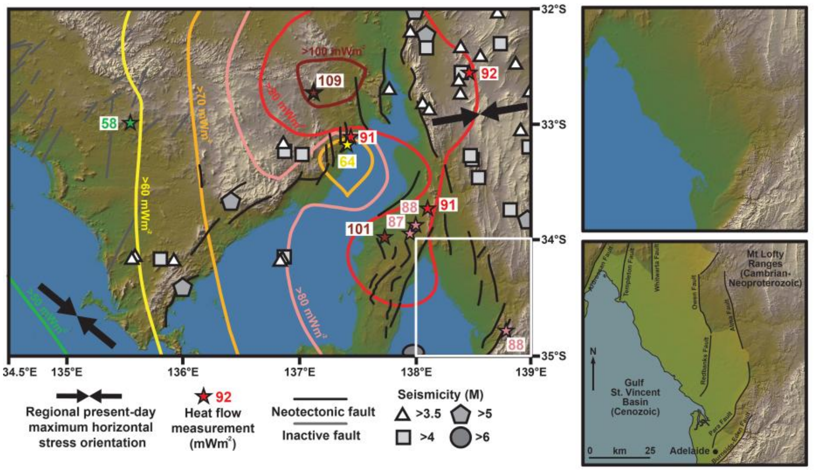

Holford et al Figure 4

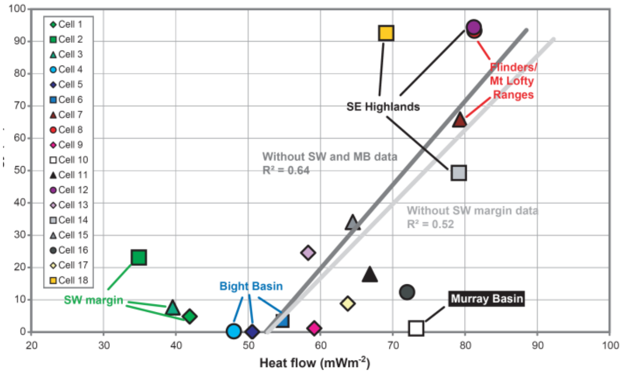

TABLE DR1. Southern Australian margin heat flow measurements.

Location/well/borehole	Basin/Region	Longitude	Latitude	Heat flow (mW m^{-2})	Error (mW m^{-2})	Reference
Moomba 17	Cooper	140.1806953	-28.1644837	102	6	Beardsmore (2005)
Moomba 50	Cooper	140.1895358	-28.0683834	103	8	Beardsmore (2005)
Moomba 15	Cooper	140.1968954	-28.1930503	95	9	Beardsmore (2005)
Big Lake 30	Cooper	140.2154599	-28.2662809	89	7	Beardsmore (2005)
Moomba North 1	Cooper	140.2418463	-28.0668718	103	8	Beardsmore (2005)
Moomba North 2	Cooper	140.2576737	-28.0486689	106	8	Beardsmore (2005)
Big Lake 30	Cooper	140.2612592	-28.2457971	87	7	Beardsmore (2005)
Big Lake 2	Cooper	140.2871892	-28.2280524	102	8	Beardsmore (2005)
Big Lake 32	Cooper	140.2904558	-28.2195662	105	8	Beardsmore (2005)
Big Lake 34	Cooper	140.3097083	-28.2193966	101	8	Beardsmore (2005)
Big Lake 35	Cooper	140.3150137	-28.2128021	103	8	Beardsmore (2005)
Big Lake 1	Cooper	140.333619	-28.2081436	102	8	Beardsmore (2005)
Namur 1	Cooper	140.4311982	-28.184726	113	10	Beardsmore (2005)
Mt Magnet	Yilgarn Craton	118	-28	54	8	Cull (1982)
Bullfinch	Yilgarn Craton	119.32	-31.23	50	8	Cull (1982)
Ravensthorpe	Yilgarn Craton	120	-33.67	39	2	Cull (1982)
Woolgangie	Yilgarn Craton	120.5	-31.25	41	1	Cull (1982)
Coolgardie	Yilgarn Craton	121.17	-30.95	33	3	Cull (1982
Kalgoorlie	Yilgarn Craton	121.43	-30.68	34	2	Cull (1982)
Wanamay	Yilgarn Craton	121.53	-31.68	34	1	Cull (1982)
Widgiemool	Yilgarn Craton	121.58	-31.52	32	3	Cull (1982)
Norseman	Yilgarn Craton	121.62	-32.33	37	4	Cull (1982)
Kambalda	Yilgarn Craton	121.68	-31.2	31	2	Cull (1982)
Mt Windara	Yilgarn Craton	122.23	-28.5	40	4	Cull (1982)
Fraser Ring	Yilgarn Craton	122.95	-32	29	1	Cull (1982)
Maralinga	Eucla Basin	131.6	-30.17	54	4	Cull (1982)
Tarcoola	Gawler Craton	134.5	-30.62	49	4	Cull (1982)
Wudinna	Eyre Peninsula	135.55	-32.98	58	8	Cull (1982)
Iron Knob	Eyre Peninsula	137.13	-32.72	109	10	Cull (1982)
Bendigo St	Eyre Peninsula	137.49	-33.2	64	1	Cull (1982)
Whyalla	Eyre Peninsula	137.5	-33.17	91	2	Cull (1982)
Kadina	Flinders Ranges	137.75	-33.97	101	4	Cull (1982)
Bute	Flinders Ranges	137.97	-33.93	87	8	Cull (1982)
Bute	Flinders Ranges	138.02	-33.87	88	2	Cull (1982)
Ediacara	Flinders Ranges	138.12	-30.6	96	8	Cull (1982)
Wokurna	Flinders Ranges	138.12	-33.72	91	4	Cull (1982)
Carrieton	Flinders Ranges	138.48	-32.55	92	4	Cull (1982)
Stockyard	Flinders Ranges	138.8	-34.77	88	8	Cull (1982)
Kanmantoo	Flinders Ranges	139.25	-35.08	88	3	Cull (1982)
Mt McTagga	Flinders Ranges	139.3	-30.45	101	8	Cull (1982)
Parabarana	Flinders Ranges	139.72	-29.98	126	8	Cull (1982)
Radium Hill	Broken Hill	140.5	-32.5	75	4	Cull (1982)
Mt Gambier	Otway	140.86	-37.75	92	3	Cull (1982)
Motooroo	Broken Hill	140.93	-32.25	68	2	Cull (1982)
Broken Hill	Broken Hill	141.47	-31.95	80	1	Cull (1982)
Heywood	Otway	141.53	-38.13	50	3	Cull (1982)
Portland	Otway	141.58	-38.38	50	1	Cull (1982)
Braxenholm	Otway	141.8	-37.87	55	1	Cull (1982)
Stawell	SE Highlands	142.78	-37.05	119	12	Cull (1982)
Timboon	Otway	142.98	-38.47	71	5	Cull (1982)
Castlemaine	SE Highlands	144.22	-37.05	121	11	Cull (1982)
Sorrento	Otway	144.73	-38.35	55	10	Cull (1982)
Roseberry	Tasmania	145.57	-41.77	104	6	Cull (1982)
Olga Ridge	Tasmania	145.78	-42.77	57	11	Cull (1982)
Cobar	SE Highlands	145.8	-31.43	83	13	Cull (1982)
Berrigan	SE Highlands	145.8	-35.7	73	1	Cull (1982)
G Lake/Dee	Tasmania	146.6	-41.97	83	5	Cull (1982)
Ardlethan	SE Highlands	146.85	-34.34	99	5	Cull (1982)
Glenorchy	Tasmania	147.25	-42.83	87	8	Cull (1982)
Storey Ck	Tasmania	147.75	-41.67	159	2	Cull (1982)
Snowy Mts	SE Highlands	148.3	-36.4	84	8	Cull (1982)
Stromlo	SE Highlands	149	-35.28	86	1	Cull (1982)
Hall	SE Highlands	149.03	-35.08	69	3	Cull (1982)
Canberra	SE Highlands	149.15	-35.3	73	3	Cull (1982)
Cpt Flat	SE Highlands	149.45	-35.6	101	4	Cull (1982)
Woodlawn	SE Highlands	149.52	-34.98	60	2	Cull (1982)
Apsley	SE Highlands	149.57	-33.57	63	1	Cull (1982)
Tarago	SE Highlands	149.57	-35.07	80	4	Cull (1982)
Narooma	SE Highlands	150.1	-36.25	54	2	Cull (1982)
Dromedary 1	SE Highlands	150.1	-36.3	47	1	Cull (1982)
Dromedary 2	SE Highlands	150.1	-36.3	43	1	Cull (1982)
Moruya	SE Highlands	150.12	-35.9	51	1	Cull (1982)
Mallandool	SE Highlands	150.73	-34.32	88	8	Cull (1982)
Nebo	SE Highlands	150.75	-34.42	80	4	Cull (1982)
Loddon	SE Highlands	150.77	-34.23	88	2	Cull (1982)
Scone	SE Highlands	150.82	-32.08	50	1	Cull (1982)
Cape Banks	SE Highlands	151.25	-34	71	1	Cull (1982)
Chowilla 1	Murray	140.78192	-33.741806	51	n/a	Eden Energy (07/17/08)
Jerboa 1	Bight	127.602213	-33.502787	48	13	Goutorbe et al. (2008)
Potoroo 1	Bight	130.7700067	-33.3857208	49	11	Goutorbe et al. (2008)
Columbia 1	Bight	133.8859709	-33.49273539	50	14	Goutorbe et al. (2008)

Greenly 1	Bight	134.9314291	-35.47708958	46	11	Goutorbe et al. (2008)
Vivonne 1	Bight	136.013884	-35.891458	61	14	Goutorbe et al. (2008)
Morum 1	Otway	139.236883	-37.501061	49	12	Goutorbe et al. (2008)
Troas 1	Otway	139.390935	-37.3657	53	11	Goutorbe et al. (2008)
Sophia Jane 1	Otway	139.6187318	-37.31177969	47	18	Goutorbe et al. (2008)
Copa 1	Otway	139.75751	-37.686961	52	12	Goutorbe et al. (2008)
Breaksea Reef 1	Otway	140.613719	-38.15712	48	8	Goutorbe et al. (2008)
Discovery Bay 1	Otway	141.0739123	-38.41045725	53	11	Goutorbe et al. (2008)
Voluta 1	Otway	141.314584	-38.428165	57	16	Goutorbe et al. (2008)
Bridgewater Bay 1	Otway	141.3647011	-38.53908422	46	9	Goutorbe et al. (2008)
Casino 1	Otway	142.7000797	-38.78847278	57	14	Goutorbe et al. (2008)
Casino 2	Otway	142.747429	-38.795524	52	13	Goutorbe et al. (2008)
Thylacine 1	Otway	142.9136487	-39.23950894	68	14	Goutorbe et al. (2008)
Geographe 1	Otway	142.928854	-39.111601	68	14	Goutorbe et al. (2008)
Minerva 1/1A	Otway	142.9547954	-38.70190497	69	14	Goutorbe et al. (2008)
Eric The Red 1	Otway	143.1823291	-39.01112897	58	14	Goutorbe et al. (2008)
Seal 1	Bass	144.882656	-39.362094	67	17	Goutorbe et al. (2008)
Cape Sorell 1	Sorell	145.030798	-42.13452728	57	11	Goutorbe et al. (2008)
Koorkah 1	Bass	145.152769	-39.631065	62	12	Goutorbe et al. (2008)
Toolka 1	Bass	145.397199	-39.40840522	55	13	Goutorbe et al. (2008)
Aroo 1	Bass	145.448002	-39.790253	60	12	Goutorbe et al. (2008)
Flinders 1	Bass	145.673215	-40.379543	75	14	Goutorbe et al. (2008)
Yolla 1	Bass	145.807052	-39.837061	63	17	Goutorbe et al. (2008)
Yolla 2	Bass	145.812036	-39.857894	54	15	Goutorbe et al. (2008)
Nangkero 1	Bass	145.979659	-40.071869	54	11	Goutorbe et al. (2008)
Tilana 1	Bass	145.979667	-39.892015	46	16	Goutorbe et al. (2008)
Dondu 1	Bass	146.218722	-39.985299	56	13	Goutorbe et al. (2008)
Chat 1	Bass	146.699927	-40.17999192	56	12	Goutorbe et al. (2008)
Durroon 1	Bass	147.213468	-40.534148	53	15	Goutorbe et al. (2008)
Torsk 1	Gippsland	147.498507	-38.4454	61	15	Goutorbe et al. (2008)
Whiptail 1A	Gippsland	147.5206096	-38.32356353	76	12	Goutorbe et al. (2008)
Speke 1	Gippsland	147.621223	-38.50808233	69	12	Goutorbe et al. (2008)
Tarra 1	Gippsland	147.703562	-38.64211808	61	12	Goutorbe et al. (2008)
Wirrah 2	Gippsland	147.825328	-38.182057	67	12	Goutorbe et al. (2008)
Orange Roughy 1	Gippsland	148.043223	-38.580983	76	16	Goutorbe et al. (2008)
Conger 1	Gippsland	148.0641432	-38.35616581	67	12	Goutorbe et al. (2008)
Hermes 1	Gippsland	148.2996815	-38.60068567	68	16	Goutorbe et al. (2008)
Teraglin 1	Gippsland	148.342969	-38.379288	46	15	Goutorbe et al. (2008)
Tuna 4	Gippsland	148.370179	-38.187623	62	11	Goutorbe et al. (2008)
Pilotfish 1	Gippsland	148.470298	-38.431359	42	14	Goutorbe et al. (2008)
Terakihi 1	Gippsland	148.546596	-38.5042	47	11	Goutorbe et al. (2008)
Billfish 1	Gippsland	148.5553289	-38.66873392	51	13	Goutorbe et al. (2008)
East Pilchard 1	Gippsland	148.561889	-38.198333	66	11	Goutorbe et al. (2008)
Blackbeak 1	Gippsland	148.5629656	-38.54943614	48	8	Goutorbe et al. (2008)
Bignose 1	Gippsland	148.602786	-38.354404	76	20	Goutorbe et al. (2008)
Great White 1	Gippsland	148.62725	-38.451944	53	11	Goutorbe et al. (2008)
Basker South 1	Gippsland	148.690582	-38.318287	57	19	Goutorbe et al. (2008)
Chimaera 1	Gippsland	148.7232467	-38.264111	63	16	Goutorbe et al. (2008)
Manta 1	Gippsland	148.7234	-38.272694	65	17	Goutorbe et al. (2008)
Jan Juc 8215	Otway	144.18	-38.39	101	n/a	Greenearth Energy (12/21/07)
Hindhaugh Creek 1	Otway	144.20078	-38.27659	72	n/a	Greenearth Energy (12/21/07)
Bellarine 1	Otway	144.21478	-38.2854	83	n/a	Greenearth Energy (12/21/07)
Geelong Flow Oil 1	Otway	144.33882	-38.29961	86	n/a	Greenearth Energy (12/21/07)
Olympic Dam RD21	Gawler Craton	136.888611	-30.437222	125	n/a	Houseman et al. (1989)
WRD2	Gawler Craton	136.888611	-30.437222	78	n/a	Houseman et al. (1989)
IDD1	Gawler Craton	136.888611	-30.437222	62	n/a	Houseman et al. (1989)
ACD3	Gawler Craton	136.888611	-30.437222	101	n/a	Houseman et al. (1989)
SGD2	Gawler Craton	136.888611	-30.437222	84	n/a	Houseman et al. (1989)
HHD1	Gawler Craton	136.888611	-30.437222	86	n/a	Houseman et al. (1989)
BD2	Gawler Craton	136.888611	-30.437222	50	n/a	Houseman et al. (1989)
Andamooka BLD1	Gawler Craton	137.166667	-30.433333	67	n/a	Houseman et al. (1989)
Tiberias	Tasmania	147.38531	-42.439827	73	n/a	KUTh Energy (08/12/08)
Kingston	Tasmania	147.57439	-41.70237	86	n/a	KUTh Energy (08/12/08)
Woodsdale	Tasmania	147.63277	-42.481968	81	n/a	KUTh Energy (08/12/08)
Fingal	Tasmania	148.08644	-41.712658	97	n/a	KUTh Energy (08/12/08)
Temple Bar	Tasmania	147.36465	-41.51873	87	n/a	KUTh Energy (06/20/08)
Epping	Tasmania	147.39967	-41.70764	62	n/a	KUTh Energy (06/20/08)
Ben Lomond	Tasmania	147.55876	-41.53176	97	n/a	KUTh Energy (06/20/08)
Tower Hill	Tasmania	147.88689	-41.550597	83	n/a	KUTh Energy (06/20/08)
Elizabeth 1	Tasmania	147.59715	-41.94011	94	n/a	KUTh Energy (04/28/08)
Tooms 1	Tasmania	147.81674	-42.270256	96	n/a	KUTh Energy (04/28/08)
Lake Leake 1	Tasmania	147.82855	-42.101826	92	n/a	KUTh Energy (04/28/08)
Snow 1	Tasmania	147.87886	-41.923096	92	n/a	KUTh Energy (04/28/08)
CO9-106	Southern Ocean	120.0333333	-44.28333333	30	n/a	Langseth and Taylor (1967)
BRK001	Murray	139.1610658	-35.5114753	89	17	Matthews and Beardsmore (2007)
Nunga Mia 1	Otway	139.8277471	-37.1459218	64	5	Matthews and Beardsmore (2007)
St Clair 1	Otway	140.0451391	-37.3625368	77	6	Matthews and Beardsmore (2007)
Camelback 1	Otway	140.1894216	-37.1031308	99	9	Matthews and Beardsmore (2007)
Wanda 1	Otway	140.2233226	-36.9289677	99	8	Matthews and Beardsmore (2007)
Crankshaft 1	Otway	140.2754359	-37.2575278	70	6	Matthews and Beardsmore (2007)
Lucindale 1	Otway	140.3103104	-37.0936002	123	10	Matthews and Beardsmore (2007)
STR130	Murray	140.3244159	-36.1726824	42	2	Matthews and Beardsmore (2007)
SPE013	Otway	140.487427	-37.068444	87	6	Matthews and Beardsmore (2007)
CLS013	Otway	140.5184122	-37.2782899	58	12	Matthews and Beardsmore (2007)
ROB011	Otway	140.6281838	-37.1097527	98	22	Matthews and Beardsmore (2007)
Bool Lagoon 1	Otway	140.6336831	-37.14494	88	7	Matthews and Beardsmore (2007)

WRG031	Murray	140.6850884	-36.3644646	68	3	Matthews and Beardsmore (2007)
Balnaves 1	Otway	140.7044722	-37.4473611	69	6	Matthews and Beardsmore (2007)
KLN010	Otway	140.7165152	-37.2601996	62	1	Matthews and Beardsmore (2007)
Viewbank 1	Otway	140.759049	-37.3253925	72	6	Matthews and Beardsmore (2007)
PNN003	Murray	140.7664056	-35.5933074	64	3	Matthews and Beardsmore (2007)
SHG006	Murray	140.7958589	-35.8179973	73	3	Matthews and Beardsmore (2007)
TAT027	Murray	140.898921	-36.372202	79	1	Matthews and Beardsmore (2007)
CMM082	Otway	140.9072591	-37.2264473	65	3	Matthews and Beardsmore (2007)
FID001	Murray	139.660223	-35.9666325	75	12	Matthews and Beardsmore (2007)
CRC001	Murray	140.0069688	-35.5676242	68	1	Matthews and Beardsmore (2007)
JOY019	Otway	140.4028567	-37.0438578	79	4	Matthews and Beardsmore (2007)
JOA011	Otway	140.8095608	-37.1368378	58	2	Matthews and Beardsmore (2007)
Parala	Flinders Ranges	139.7133344	-30.2097236	129	n/a	Petratherm (12/31/2006)
Horsham (VIMP3)	SE Highlands	142	-36.862	89.8	n/a	Purss and Cull (2001)
Warracknabeal (VIMP4)	SE Highlands	142.347	-36.483	97	n/a	Purss and Cull (2001)
Torrens 1	Flinders Ranges	138.06244	-31.701963	82	n/a	Torrens Energy (05/15/08)
Nazgul 1	Flinders Ranges	138.15099	-31.07464	106	n/a	Torrens Energy (05/15/08)
Sauron 1	Flinders Ranges	138.17796	-31.181122	106	n/a	Torrens Energy (05/15/08)
Gandalf 1	Flinders Ranges	138.18304	-31.304562	85	n/a	Torrens Energy (05/15/08)
Balrog 1	Flinders Ranges	138.2702	-31.265034	95	n/a	Torrens Energy (05/15/08)
Gollum 1	Flinders Ranges	138.34756	-31.14662	90	n/a	Torrens Energy (05/15/08)
Edeowie 1	Flinders Ranges	138.43137	-31.295927	70	n/a	Torrens Energy (05/15/08)
V18-74	Southern Ocean	118.7833333	-36.11666667	43	n/a	Von Herzen and Langseth (1965)
MSN-48	Southern Ocean	119.8666667	-39.3	44	n/a	Von Herzen and Langseth (1965)
V18-76	Southern Ocean	133.6666667	-37.45	48	n/a	Von Herzen and Langseth (1965)

REFERENCES

Beardsmore, G.R., 2005, Thermal modelling of the hot dry rock geothermal resource beneath GEL99 in the Cooper Basin, South Australia: Proceedings World Geothermal Congress 2005, Antalya, Turkey, 24-25 April 2005.

Cull, J.P., 1982, An appraisal of Australian heat-flow data: BMR Journal of Australian Geology and Geophysics, v. 7, p. 11-21.

Eden Energy Ltd. 17 July 2008. Australian Securities Exchange Announcement. http://www.edenenergy.com.au/pdfs/ASX_Announcement%2020080717%20%20Chowilla%20Well.pdf

Goutorbe, B., Lucazeau, F., and Bonneville, A., 2008, Surface heat flow and the mantle contribution on the margins of Australia: Geochemistry, Geophysics, Geosystems, v. 9., Q05011, doi:10.1029/2007GC001924.

Greenearth Energy Ltd. 21 December 2007. Second Supplementary Prospectus. http://www.greenearthenergy.com.au/files/GreenearthProspectus.pdf

Houseman, G.A., Cull, J.P., Muir, P.M., and Paterson, H.L., 1989, Geothermal signatures and uranium ore deposits on the Stuart Shelf of South Australia: Geophysics, v. 54, p. 158-170.

KUTh Energy Ltd. 28 April 2008. Australian Securities Exchange Announcement. http://www.kuthenergy.com/index.php?item=file&target=heatflowapril

KUTh Energy Ltd. 20 June 2008. Australian Securities Exchange Announcement. http://www.kuthenergy.com/index.php?item=file&target=newgeothermalprovince

KUTh Energy Ltd. 12 August 2008. Australian Securities Exchange Announcement. http://www.kuthenergy.com/index.php?item=file&target=Aug08HeatFlowResults

Langseth, M.G., and Taylor, P.T., Recent heat flow measurements in the Indian Ocean: Journal of Geophysical Research, v. 72, p. 6249-6460.

Matthews, C., and Beardsmore, G., 2007, New heat flow data from south-eastern South Australia: Exploration Geophysics, v. 28, p. 260-269, doi:10.1071/EG07028.

Petratherm Ltd. 31 December 2006. Report for the quarter ending 31 December 2006. http://www.petratherm.com.au/_literature_37674/Quarterly_Report_-_Dec_06

Purss, M.B.J., and Cull, J., 2001, Heat-flow data in western Victoria: Australian Journal of Earth Sciences, v. 48, p. 1-4.

Torrens Energy Ltd. 15 May 2008. Australian Securities Exchange Announcement. http://www.torrensenergy.com/announcements/080515_parachilna.pdf

Von Herzen, R.P., and Langseth, M.G., 1965, Present status of oceanic heat-flow measurements, *in* Ahrens, T., ed., Physics and Chemistry of the Earth, vol. 6: Pergamon Press, New York, p. 365-407.

APPENDIX DR1. Southern Australian margin earthquake database.

To quantify the amount of seismic energy released during active deformation of the southern Australian margin we used Geoscience Australia's earthquake database, full details of which are provided by Leonard (2008). First, we selected all earthquakes that occurred within eighteen 3° x 3° cells that reflect the geometry of the margin (shown in Figure 2) between January 1900 and April 2007. We then excluded all earthquakes that fell outside the catalogue completeness levels determined by Leonard (2008). These completeness levels, modified to reflect the time span of earthquakes used in this study (i.e. 1900-2007) are as follows:

Region	**1.5**	**2.0**	**2.5**	**3.0**	**3.5**	**4.0**	**4.5**	**5.0**	**5.5**
South Australia	1980	1970			1965	1960	1900		
Southeast Australia	1975*	1970		1960		1955		1900	
Rest of Australia					1980	1970	1965	1960	1910

*Southeast Australia cut off levels have increased to 2.0-2.5 since 1995.

Finally, the remaining earthquakes were screened to remove duplicates (i.e. the same earthquakes recorded by more than one state or national geological surveys) and probable aftershocks.

We estimated the amount of seismic energy released in each 3° x 3°cell using an empirical relationship that relates seismic energy to earthquake magnitude:

$$\log E_S = 1.5M_S + 4.8$$

where E_S is the radiated seismic energy (Joules) and M_S is the measured surface wave magnitude (Scholz, 2002).

This relationship is appropriate for determination of seismic energy or moment release for earthquakes that have surface wave magnitude of <7.5 (Scholz, 2002) (only a handful of southern margin earthquakes have magnitudes >6 (Leonard, 2008)).